Infrared Physics and Technology 108 (2020) 103378

Contents lists available at ScienceDirect

Infrared Physics & Technology

journal homepage: www.elsevier.com/locate/infrared

Passively Q-switched mode-locked $Nd:GdTaO_4$ laser by rhenium diselenide saturable absorber operated at 1066 nm

Rui Wang*, Yuanyang Li, Luwei Zhang, Tao Sun

Changchun Institute of Optics, Fine Mechanics and Physics, Chinese Academy of Sciences, Changchun 130033, China

State Key Laboratory of Laser Interaction with Matter, Changchun Institute of Optics, Fine Mechanics and Physics, Chinese Academy of Sciences, Changchun 130033, China

ARTICLE INFO

Keywords:
Q-switched mode-locked
Rhenium diselenide
$Nd:GdTaO_4$

ABSTRACT

We demonstrate the fabrication process of rhenium diselenide ($ReSe_2$) saturable absorber (SA) and its application for passively Q-switched mode-locked $Nd:GdTaO_4$ laser. The characterization of this SA was described in detail. The modulation depth of the $ReSe_2$ nanosheet was 11.4%. Under the pump power of 4 W, the maximum average output power of 0.209 W was obtained with optical conversion efficiency of 5.2%. The estimated shortest mode-locked pulse width was about 447 ps. Our results show that the shorter pulse width can be obtained by $ReSe_2$ SA at 1066 nm.

1. Introduction

Two-dimensional (2D) nanosheets with excellent physical especially in optics and chemical properties could be used as functional devices both for the passively modulators and active modulators [1–5]. The unique band structure of strong covalent bonds in layers and weak van der Waals interaction between layers make the few-layer 2D materials could be easily obtained from crystals [6–8]. Recently, $ReSe_2$ nanosheets were found to be a promising saturable absorber (SA) for ultrafast lasers [9–11]. The few-layer $ReSe_2$ nanosheet (6–8 layers) with band gap of 1.28 eV, the corresponding absorption wavelength is 970 nm [12]. Therefore, it could be used as SA at the wavelength around 1 μm. In addition, the $ReSe_2$ nanosheet shows a strong in-plane anisotropy due to the stable distorted 1T′ phase [13–16]. Compared with other materials, $ReSe_2$ nanosheet shows larger nonlinear optical response and damage threshold, which makes it more suitable for saturable absorbers (SAs) in lasers.

Compared with widely used crystals for solid-state lasers, $Nd:GdTaO_4$ crystal shows a wider absorption around 808 nm, which makes it less sensitivity to the changing pumping wavelength. In addition, the low symmetry and high photoluminescence efficiency were also the advantages for a gain medium in solid-state lasers. Therefore, the $Nd:GdTaO_4$ crystal is a good candidate for mode-locked lasers [17,18].

There are various methods for the preparation of small-layer 2D material samples, such as chemical vapor deposition, magnetic sputtering, mechanical stripping, physical vapor deposition and liquid phase stripping. Among them, the liquid phase stripping method has many advantages: simple fabrication method, the number of nanosheet layers can be largely controlled by controlling the centrifugation time, the nanosheet orientation uniformity is better by controlling the ultrasound rate and time. Thus, this method was always chosen to prepare 2D material samples [19].

In this paper, we proposed and experimentally demonstrated a passively Q-switched mode-locked $Nd:GdTaO_4$ laser with $ReSe_2$ SA operated at 1066 nm. Firstly, the characterization of this SA was described in detail. The linear transmission spectrum, nonlinear transmission spectrum, the AFM and SEM photographs were used to show the surface morphology and optical properties. Secondly, the passively Q-switched mode-locked operation in $Nd:GdTaO_4$ laser also be reported. Under the pump power of 4 W, the maximum average output power of 0.209 W was obtained with the optical conversion efficiency of 5.2%. Experimental results show that $ReSe_2$ nanosheet with excellent optical saturable absorption property could be promising material for SAs in ultrafast solid-state lasers especially for 1 μm lasers.

2. Preparation and characterization of $ReSe_2$ SA

We used liquid-phase stripping method to prepare $ReSe_2$ SA. First, 0.2 g of the $ReSe_2$ powder with particle diameter less than 30 μm was added into 30 mL absolute ethyl alcohol. Secondly, the solution was stirred by ultrasound for 300 min. Thirdly, a quartz sheet

* Corresponding author at: Changchun Institute of Optics, Fine Mechanics and Physics, Chinese Academy of Sciences, Changchun 130033, China.
E-mail address: darui99999@163.com (R. Wang).

https://doi.org/10.1016/j.infrared.2020.103378
Received 17 April 2020; Received in revised form 24 May 2020; Accepted 24 May 2020
Available online 28 May 2020

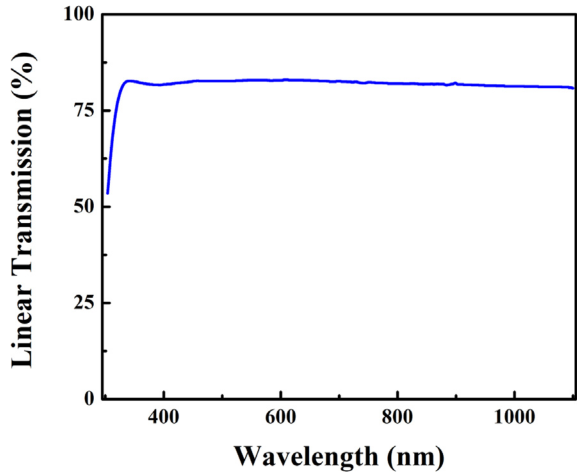

Fig. 1. UV–Vis-NIR linear transmission spectrum.

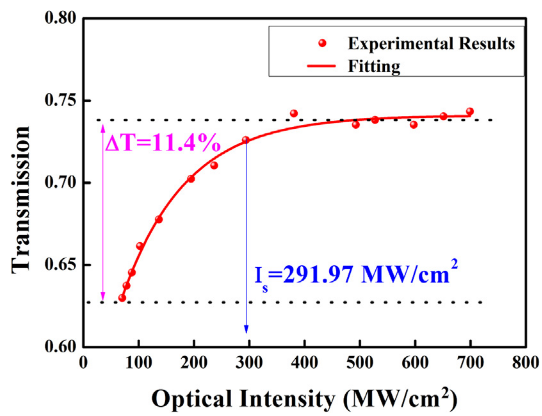

Fig. 2. Nonlinear transmission spectrum.

(20 mm × 10 mm) was submerged into the solution completely. Finally, left the quartz sheet at room temperature for 12 h.

As shown in Fig. 1, the $ReSe_2$ SA shows a broad transmission in the 400–1100 nm spectral range, and the transmissivity at 1066 nm was 81.16%. From Fig. 1, the transmissivity shows a strongly relations with the wavelength. When the wavelength below 350 nm, the transmittance drops sharply due to the strong absorption of ultraviolet high-energy photons. However, when the wavelength is higher than 350 nm, the transmittance remains basically unchanged. Our results show that the $ReSe_2$ nanosheet could be used as SA during a wide wavelength range.

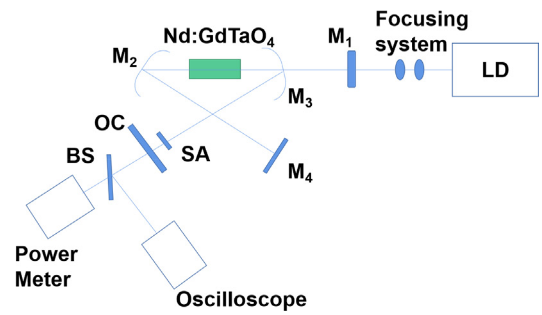

Fig. 4. Schematic setup of the $Nd{:}GdTaO_4$ laser.

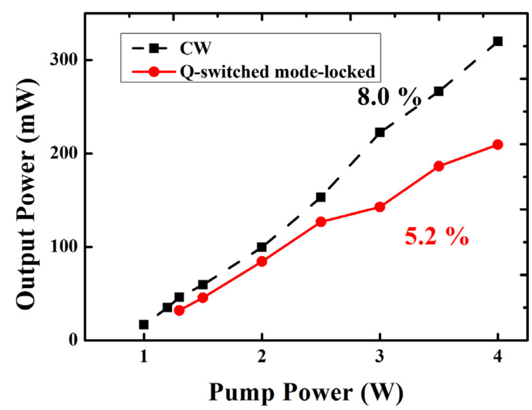

Fig. 5. Power efficiency data of the CW and Q-switched mode-locked operations.

The nonlinear transmission spectrum (See Fig. 2) was used to measure the saturation intensity and modulation depth of $ReSe_2$ SA. Indeed, the two indexes are important factors for evaluating the performance of SAs. Here, we use an ultrafast laser with pulse during time of 350 fs, central wavelength of 800 nm and pulse energy of 0.47 μJ.

The nonlinear transmission performance of the experimental data could be fitted by [17]:

$$T = 1 - T_1 - T_2 \cdot \exp\left(-\frac{I}{I_s}\right)$$

where T_1 and T_2 are non-saturable absorbance and modulation depth of SA, I and Is are laser intensity and saturation intensity of SA. After calculation, the saturation intensity and modulation depth were

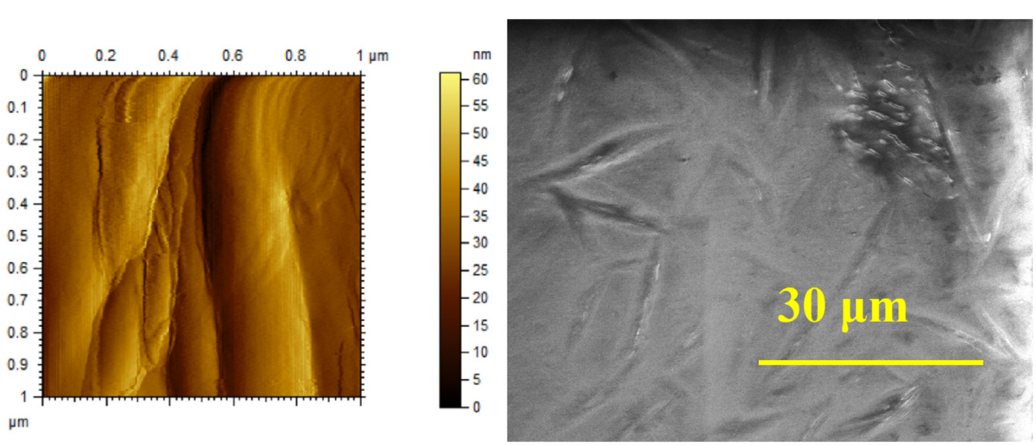

(a) AFM photograph (b) SEM photograph

Fig. 3. AFM and SEM photographs of the $ReSe_2$ nanosheet.

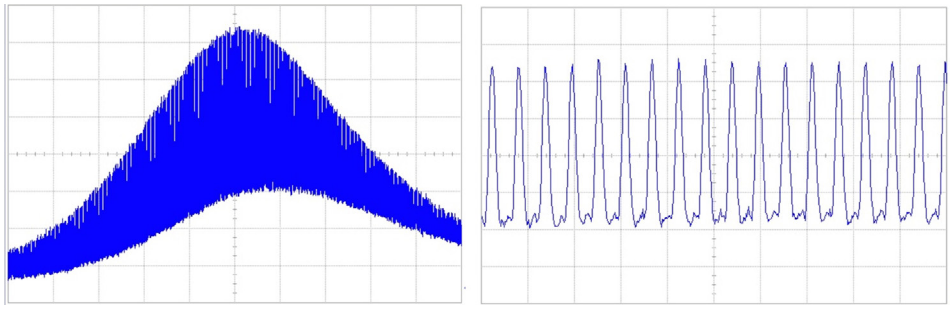

(a) Temporal shape (500ns/div) (b) pulse trains (20ns/div).

Fig. 6. Temporal shape and pulse trains of the Q-switched mode-locked $Nd:GdTaO_4$ laser.

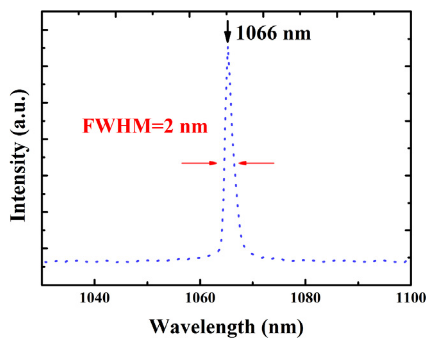

Fig. 7. Spectrum of Q-switched mode-locked $Nd:GdTaO_4$ laser.

291.97 MW/cm^2 and 11.4%, respectively.

In addition, in order to characterize the surface morphology and the number of layers of the $ReSe_2$ nanosheet, the SEM and AFM photographs were measured (see Fig. 3). Form Fig. 3, the average thickness is 10.91 nm (corresponding layers number of 11) and the size of the nanosheet is 250 nm × 300 nm.

3. Experimental setup

Fig. 4 shows the schematic setup of the $Nd:GdTaO_4$ laser. The Q-switched mode-locking laser was based on a standard X-folded cavity with the length of about 1.8 m. A fiber-coupled diode laser (LD) with the emission wavelength centered at 808 nm was used as the pump source. The dimensions of the $Nd:GdTaO_4$ crystal was 3 × 3 × 5 mm^3. M_1 and M_4 are flat mirrors (high-transmission at 808 nm and high-reflection at 1.06 μm). M_2 and M_3 are concave mirrors with the radius of curvature of 500 mm, the flat mirror OC is an output coupler with the transmissions of 3.0% at 1.06 μm. A 1:1 unpolarized beam splitter (BS) was used to divided the output laser into two beams. One part was recorded by a fast photo-detector and an oscilloscope, another part was measured by a power meter.

4. Experimental results and discussions

Firstly, CW operation was obtained with the optical conversion efficiency and the slope efficiency of 8.0% and 11.0%, respectively. The threshold pump power of CW operation was 0.85 W. After that, the $ReSe_2$ SA was set before the OC. When the pump power increased to 1.3 W, we got the Q-switched operation. With the pump power increased to 1.7 W, the Q-switched mode-locked operation was obtained. Fig. 5 shows the relationship of the laser output power versus pump power. Under the pump power of 4 W, the maximum average output power of 0.209 W was obtained with the optical conversion efficiency of 5.2% by using $ReSe_2$ SA.

Fig. 6 shows the temporal shape of a Q-switched pulse envelope and pulse trains of the Q-switched mode-locked $Nd:GdTaO_4$ laser. The mode-locked pulses inside the Q-switched envelope is quite stable with the repetition rate of 83 MHz. According to the expanded oscilloscope traces of the mode-locked pulse within the Q-switched envelope shown in Fig. 6 (b), the mode-locked pulse width can be estimated by the formula [17]:

$$t_{real}^2 = t_{measure}^2 - t_{probe}^2 - t_{oscilloscope}^2,$$

Here, t_{real} is the real rise time of the pulse, $t_{measure}$ is the measured rise time, t_{probe} is the rise time of the probe and $t_{oscilloscope}$ is the rise time of the oscilloscope.

In this work, the average rise time of the mode-locked pulses is 0.53 ns. The rise time of oscilloscope is 0.35 ns and the rise time of the probe is about 0.175 ns. Assuming that the pulse width is approximately 1.25 times more than the rise time, the estimated mode-locked pulse width is about 447 ps.

The output spectrum of Q-switched mode-locked $Nd:GdTaO_4$ laser is shown in Fig. 7. With $ReSe_2$ SA inserting in the laser cavity, laser line peaked at 1066 nm with full width at half maximum (FWHM) of 2 nm had been demonstrated, which is fully consistent with the fluorescence spectrum shown in Ref. [17].

Some results of the $ReSe_2$ SAs based lasers were listed in Table 1. Among these works, only this work had shown the $ReSe_2$ saturable absorber in 1 μm solid-state lasers. In Ref. [9], the laser wavelength was

Table 1
Results of the $ReSe_2$ SAs based lasers. QS: Q-switched, ML: mode-locked.

Lasers	Gain medium	Max Output power	Shortest pulse width	Modulation depth	Wavelength	Ref
QS	Ytterbium-doped fiber	5.6 mW	2.87 μs	28.75%@980 nm	1.06 μm	[9]
ML	Waveguide laser	~100 mW	29 ps	8.5%@550 nm 2.5%@1030 nm	1.06 μm	[10]
QS	Tm:YLF	180 mW	1.61 μs	6.86%@1910 nm	1.9 μm	[11]
QS	Er:YAP	526 mW	202.8 ns	7.5% @3 μm	3 μm	[13]
QS	Tm:YLF	862 mW	527.9 ns	–	2 μm	[14]
QS	Tm:YLF	486 mW	716 ns	1.3%@1030 nm	2.3 μm	[15]
QS	$Nd:Y_3Al_5O_{12}$	~600 mW	1.08 μs	–	1.06 μm	[16]
QSML	$Nd:GdTaO_4$	209 mW	447 ps	11.4%@800 nm	1.06 μm	This work

closer (980 nm) to the band gap of the few-layer $ReSe_2$ nanosheet, and the modulation depth is larger than our work, but we obtained the max laser output power for Q-switched mode-locked operation.

5. Conclusions

Summarizing, we have demonstrated a passively Q-switched mode-locked $Nd:GdTaO_4$ laser using $ReSe_2$ SA. Under the pump power of 4 W, the maximum average output power of 0.209 W was obtained with the optical conversion efficiency of 5.2%. The estimated shortest mode-locked pulse width is about 447 ps. The $ReSe_2$ with good optical saturable absorption property could be promising material for SAs at the operation wavelength around 1 μm.

Funding

This work is supported by the Jilin Scientific and Technological Department Program (Grant No. 20190302050GX).

Declaration of Competing Interest

The authors declared that there is no conflict of interest.

References

[1] W.W. Zhang, J.Q. Sun, J. Wang, L. Liu, Multiwavelength mode-locked fiber-ring laser based on reflective semiconductor optical amplifiers, Photon. Technol. Lett., IEEE 19 (19) (2007) 1418–1420.

[2] J. Xia, Y.F. Lü, H.L. Liu, X.Y. Pu, Diode-pumped $Pr^{3+}:LiYF_4$ visible dual-wavelength laser, Opt. Commun. 334 (2015) 160–163.

[3] Q. Song, G.J. Wang, B.Y. Zhang, W.J. Wang, M.H. Wang, Q.L. Zhang, G.H. Sun, Y. Bo, Q.J. Peng, Diode-pumped passively dual-wave length Q-switched Nd:GYSGG laser using graphene oxide as the saturable absorber, Appl. Opt. 54 (10) (2015) 2688–2692.

[4] Y.J. Huang, Y.S. Tzeng, C.Y. Tang, S.Y. Chiang, H.C. Liang, Y.F. Chen, Efficient high-power terahertz beating in a dual-wavelength synchronously mode-locked laser with dual gain media, Opt. Lett. 39 (6) (2014) 1477–1480.

[5] H. Zhang, X. Chen, Q. Wang, P. Li, Dual-wavelength actively Q-switched diode-end-pumped ceramic $Nd:YAG/BaWO_4$ Raman laser operating at 1240 and 1376 nm, Laser Phys. Lett. 11 (10) (2014) 105806.

[6] H.T. Huang, J.L. He, B.T. Zhang, J.F. Yang, J.L. Xu, C.H. Zuo, X.T. Tao, $V^{3+}:YAG$ as the saturable absorber for a diode-pumped quasi-three-level dual-wavelength Nd:GGG laser, Opt. Express 18 (4) (2010) 3352–3357.

[7] S.D. Liu, L.H. Zheng, J.L. He, J. Xu, X.D. Xu, L.B. Su, K.J. Yang, B.T. Zhang, R.H. Wang, X.M. Liu, Passively Q-switched $Nd:Sc_{0.2}Y_{0.8}SiO_5$ dual-wavelength laser with the orthogonally polarized output, Opt. Express 20 (20) (2012) 22448–22453.

[8] N. Zhang, T. Zhang, Y. Wang, et al., Compact stable passively Q-switched $Nd:YVO_4$ laser with tungsten disulfide saturable absorber, Optik 127 (19) (2016) 7689–7693.

[9] N. Wang, B.L. Lu, X.Y. Qi, et al., Passively Q-switched ytterbium-doped fiber laser with $ReSe_2$ saturable absorber, Opt. Laser Technol. 116 (2019) 300–304.

[10] Z. Li, N. Dong, Y. Zhang, et al., Invited Article: Mode-locked waveguide lasers modulated by rhenium diselenide as a new saturable absorber, APL Photon. 3 (8) (2018) 080802.

[11] C. Li, Y. Leng, J. Huo, $ReSe_2$ as a saturable absorber in a Tm-doped yttrium lithium fluoride (Tm:YLF) pulse laser, Chin. Opt. Lett. 17 (1) (2019) 011402.

[12] Q. Song, L. Chai, W. Liu, et al., THz polarization-sensitive characterization of a large-area multilayer rhenium diselenide nanofilm, Nanotechnology 30 (50) (2019) 505203.

[13] Y. Yao, N. Cui, Q. Wang, et al., Highly efficient continuous-wave and $ReSe_2$ Q-switched 3 μm dual-wavelength Er:YAP crystal lasers, Opt. Lett. 44 (11) (2019) 2839–2842.

[14] S. Wang, H. Huang, X. Liu, et al., Rhenium diselenide as the broadband saturable absorber for the nanosecond passively Q-switched thulium solid-state lasers, Opt. Mater. 88 (2019) 630–634.

[15] S. Wang, H. Huang, H. Chen, et al., High efficiency nanosecond passively Q-switched 2.3 μm Tm: YLF laser using a $ReSe_2$-based saturable output coupler, OSA Continuum 2 (5) (2019) 1676–1682.

[16] Y. Xue, L. Li, B. Zhang, et al., $ReSe_2$ passively Q-switched $Nd:Y_3Al_5O_{12}$ laser with near repetition rate limit of microsecond pulse output, Opt. Commun. 445 (2019) 165–170.

[17] Q. Song, B. Zhang, G. Wang, et al., Tungsten disulfide-graphene oxide as saturable absorber for passively Q-switched mode-locked $Nd:GdTaO_4$ laser at 1066 nm, Opt. Commun. 406 (2018) 76–79.

[18] M.X. Li, G.Y. Jin, Y. Li, Diode-pumped passively Q-switched $Nd:GdTaO_4$ laser based on tungsten disulfide nanosheets saturable absorber at 1066 nm, Infrared Phys. Technol. 90 (2018) 195–198.

[19] Q. Song, L. Chai, W. Liu, et al., THz polarization-sensitive characterization of a large-area multilayer rhenium diselenide nanofilm, Nanotechnology 50 (30) (2019) 505203.